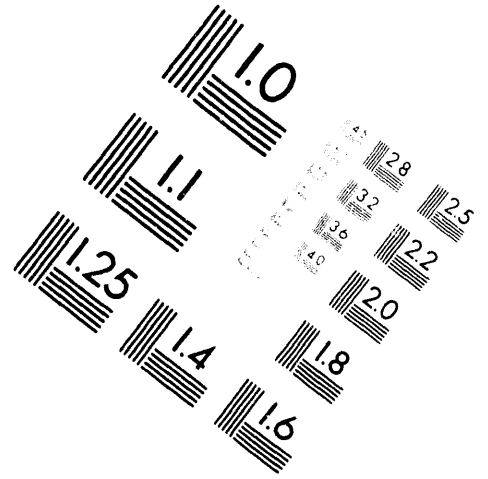
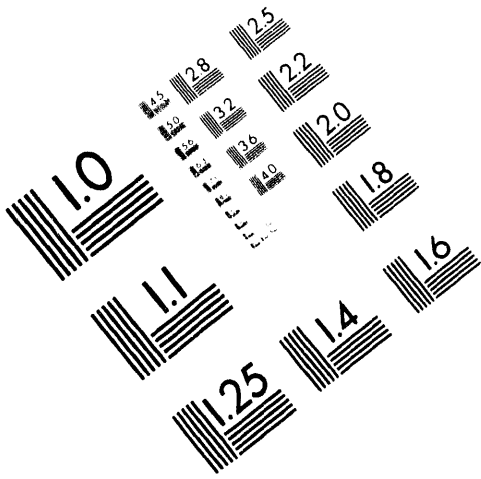




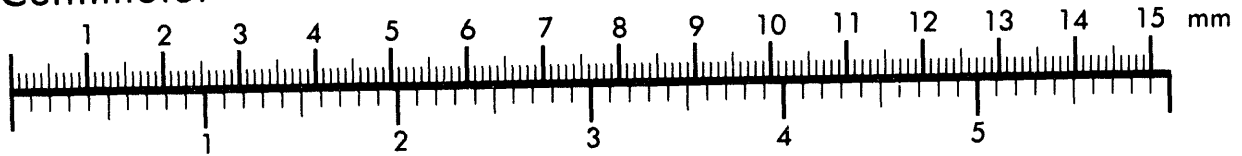
AIM

Association for Information and Image Management

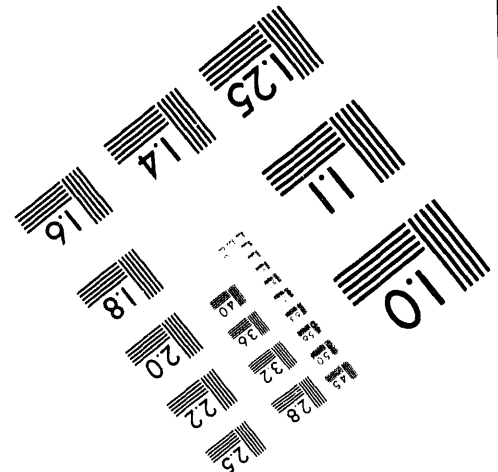
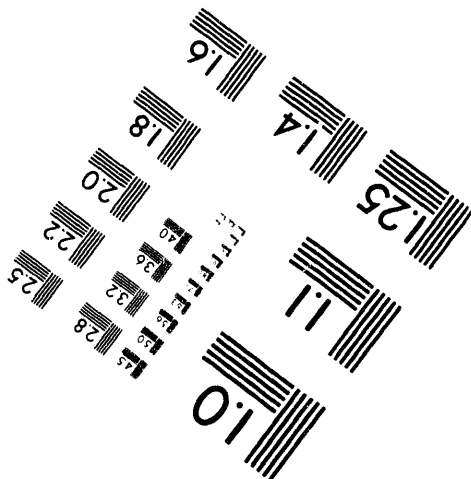
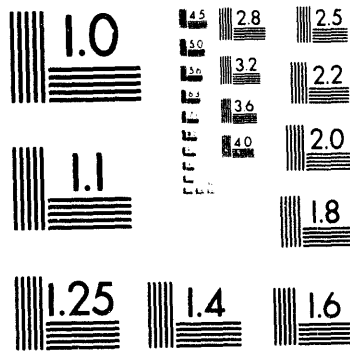
1100 Wayne Avenue, Suite 1100
Silver Spring, Maryland 20910
301/587-8202



Centimeter



Inches



MANUFACTURED TO AIM STANDARDS
BY APPLIED IMAGE, INC.

1 of 1

1
orig-140635--13

"The submitted manuscript has been authored by a contractor of the U.S. Government under contract DE-AC05-84OR21400. Accordingly, the U.S. Government retains a nonexclusive, royalty-free license to publish or reproduce the published form of this contribution, or allow others to do so, for U.S. Government purposes."

IMPURITY BEHAVIOR DURING ION-BERNSTEIN WAVE HEATING IN PBX-M*

R. C. Isler, A. P. Post-Zwicker

*Fusion Energy Division, Oak Ridge National Laboratory
Oak Ridge, Tennessee 37831, USA*

S. F. Paul, W. Tighe, M. Ono, B. P. LeBlanc, R. Bell, H. W. Kugel, R. Kaita

*Princeton Plasma Physics Laboratory
Princeton, New Jersey 08543, USA*

* Work sponsored by the Office of Fusion Energy, U. S. Department of Energy, under contracts No. DE-AC05-84OR21400 with Martin Marietta Energy Systems Inc. and No. DE-ACO2-76-CHO-33073 with the Princeton Plasma Physics Laboratory.

MASTER

ps

IMPURITY BEHAVIOR DURING ION-BERNSTEIN WAVE HEATING IN PBX-M

R. C. Isler, A. P. Post-Zwicker
Fusion Energy Division, Oak Ridge National Laboratory
Oak Ridge, Tennessee 37831, USA

S. F. Paul, W. Tighe, M. Ono, B. P. LeBlanc, H. W. Kugel, R. Kaita
Princeton Plasma Physics Laboratory
Princeton, New Jersey 08543, USA

1. Introduction

Ion-Bernstein-wave heating (IBWH) has been tested in several tokamaks. In some cases the results have been quite positive, producing temperature increases [1-4] and also improving both energy and particle confinement times [1-5], whereas in others, no distinctive changes were observed [6]. Most recently, IBWH has been utilized in the Princeton Beta Experiment-Modified (PBX-M) where the long-range goal is the achievement of operation in the second stable region by current and pressure profile control. Investigations have been performed in this machine using IBWH as the sole source of auxiliary power or using IBWH in conjunction with neutral-beam injection (NBI) or with lower-hybrid current drive (LHCD). Impurity studies seem particularly important for IBWH since not only have influxes often been observed to increase, but the global impurity confinement time has also been shown to lengthen as the confinement of the working gas improves. We present here a set of characteristic experimental results regarding the impurity behavior in PBX-M; in general, these are consonant with previous observations in other tokamaks.

2. IBW without NBI

In PBX-M it is usually observed that influxes of both low-Z and high-Z impurities increase during IBW injection in all types of operation, although the rates can be minimized by boronization of the vacuum vessel. For example, 340 kW of IBWH power can raise the iron and nickel concentrations by more than an order of magnitude above the levels detected without such auxiliary heating. The central confinement of the working gas also increases, as evidenced by the narrowing of the electron density profiles [4]. Figures 1-4 illustrate typical behavior of the radiated power and of the spectral lines during IBWH unaccompanied by NBI. The radiated power profile, as determined from a 15 channel bolometer array, tends to be hollow prior to the introduction of IBWH at 350 ms but becomes continually more peaked until a soft disruption occurs at 665 ms. The peripheral carbon and oxygen emissions grow by factors of 5 while the metals increase to the point where their lines are the dominant features in the vacuum ultraviolet spectrum. The data indicate that the strong increases in radiation from ions such as Fe XVI and Ni XVIII occur not only because of the increased influx but also as a result of the impurities becoming more centrally concentrated. This inference is based on comparing the strength of the unresolved lines from low ionization stages in the region around 200 Å to the strengths of the sodium-like and magnesium-like ions. The former increase by about a factor of 5 during IBWH while the latter rise by factors of at least 20.

3. IBW with NBI

Two distinct behaviors of the impurity transport are observed when IBWH is used in conjunction with NBI depending on whether the discharges are in the L-mode or H-mode.

In a typical L-mode discharge it is observed that 2.5 MW of NBI raises the radiation from metallic ions by about a factor of 2 over the levels observed with ohmic heating alone. The addition of 340 kW of IBWH further increases the metallic emissions by about another factor of 5, but the transport coefficients are not distinctly altered. That is, no central impurity buildup is induced; the plasma remains in the L-mode. If a discharge makes a transition to an H-mode during NBI, the impurity confinement time appears to increase at the onset, but strong central peaking of the radiation and of the metal profiles does not occur (although such an evolution has been observed in H-modes in PBX-M under different operating conditions [7]). However, the addition of IBWH dramatically alters the radiation pattern as the losses increase by a factor of 4, and the profile becomes very narrow; the electron temperature profile frequently evolves to a flat or slightly hollow shape in these cases. These observations are illustrated by Figs 5 and 6, which show the effects of 410 kW of IBWH in a discharge with 1.5 - 2.5 MW of NBI. Shortly after the beams are introduced at 350 ms the plasma makes a transition to the H-mode, and emissions from the peripheral ions, such as O V and C III drop as the electron temperature gradient steepens. The signals then rise to pre-H-mode levels as the IBWH apparently induces a greater influx of impurities starting around 450 ms.

In contrast, the metallic emissions show only minor changes until IBWH is initiated; the intensities of lines of Fe XVI and Ni XVIII then grow rapidly up to 525 ms. The subsequent sharp drop in signal strength appears to occur because of the strong pinch that compresses the iron and nickel toward the center rather than being caused by a decreasing influx. This interpretation is evident from the Fe XXIII and Ni XXV resonance lines (not depicted) which increase during this interval, although the central temperature is decreasing somewhat. Late in the discharge the behavior reverses most likely because of cooling of the plasma. The tendency toward central peaking of impurities is also observed in the profiles of O⁸⁺ ions as deduced from charge-exchange excitation (CXE). The circles in Figs 7(a) and 7(b) illustrate measurements of the 2977 Å line before and after the IBWH is started (the magnetic axis is at 165 cm). Clearly the peak moves inward during IBWH. The solid lines in these figures are fittings calculated from an impurity code in which the transport coefficients have been adjusted to give a reasonably accurate match to the data. The fully ionized oxygen profiles that produce the fittings are illustrated in Fig. 7(c). From these it can be seen that the impurity pinching during IBWH is also evident for the low-Z ions.

Acknowledgement: This work was sponsored by the Office of Fusion Energy, U. S. Department of Energy, under contracts No. DE-AC05-84OR21400 with Martin Marietta Energy Systems Inc. and No. DE-ACO2-76-CHO-33073 with the Princeton Plasma Physics Laboratory.

References

- [1] M. Ono *et al.*, Phys. Rev. Lett. **54** (1985) 2339.
- [2] J. D. Moody *et al.*, Phys. Rev. Lett. **60** (1988) 298.
- [3] M. Ono *et al.*, Phys. Rev. Lett. **60** (1988) 294.
- [4] B. P. LeBlanc, Bull. Am. Phys. Soc. **38** (1993) 1959.
- [5] T. Seki *et al.*, Nucl. Fusion **32** (1992) 2189.
- [6] R. I. Pinsky *et al.*, Nucl. Fusion **33** (1993) 777.
- [7] S. F. Paul *et al.*, J. Nucl. Mat. **196-198** (1992) 503.

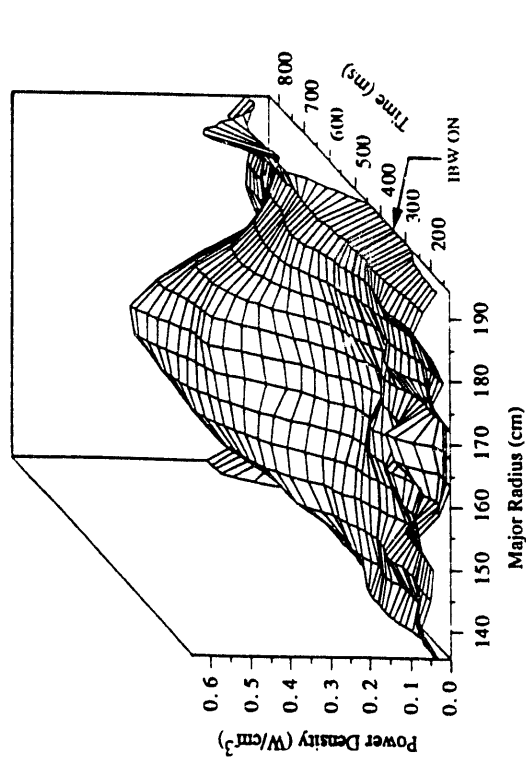


Fig. 1. Profiles of radiated power with 180 kW IBWH starting at 350 ms.

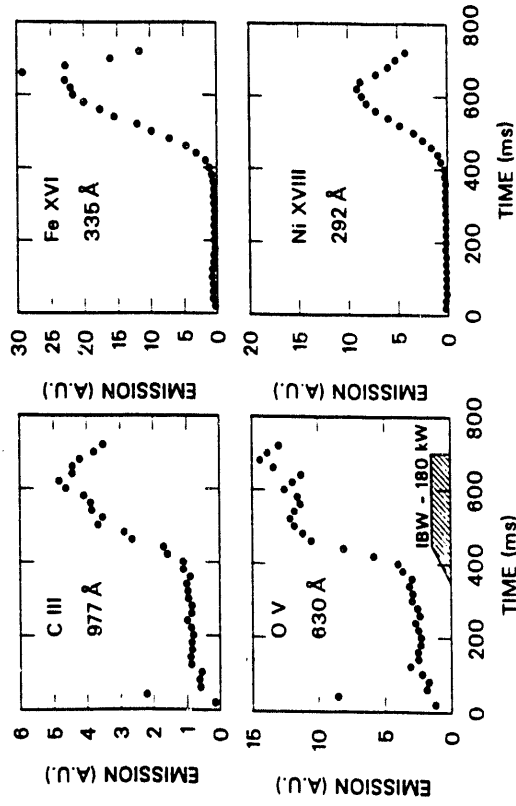


Fig. 2. Time-dependent impurity emission during IBWH.

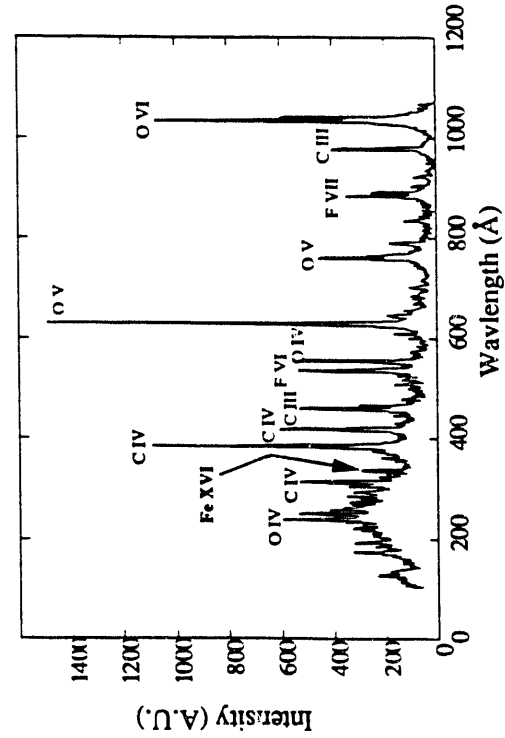


Fig. 3. Vacuum ultraviolet spectrum before IBWH.

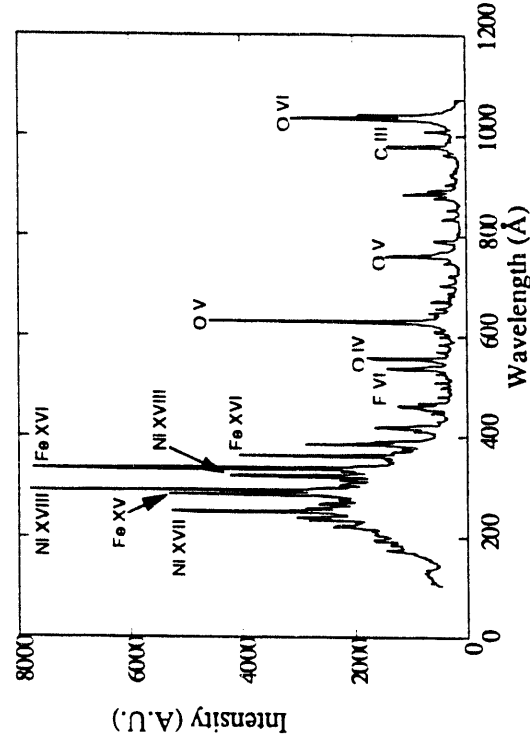


Fig. 4. Vacuum ultraviolet spectrum after 300 ms of IBWH.

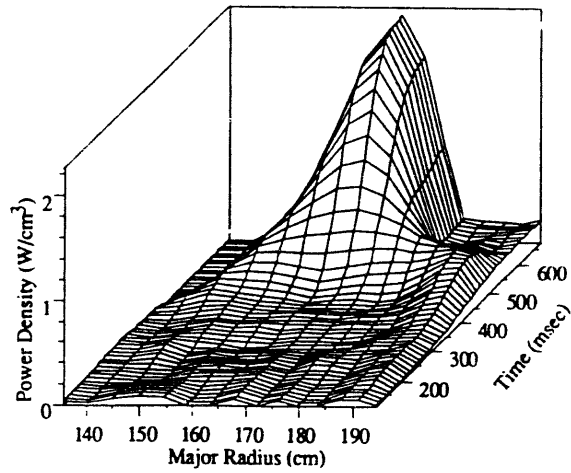


Fig. 5. Profiles of radiated power with 410 kW IBWH introduced into an H-mode plasma at 450 ms.

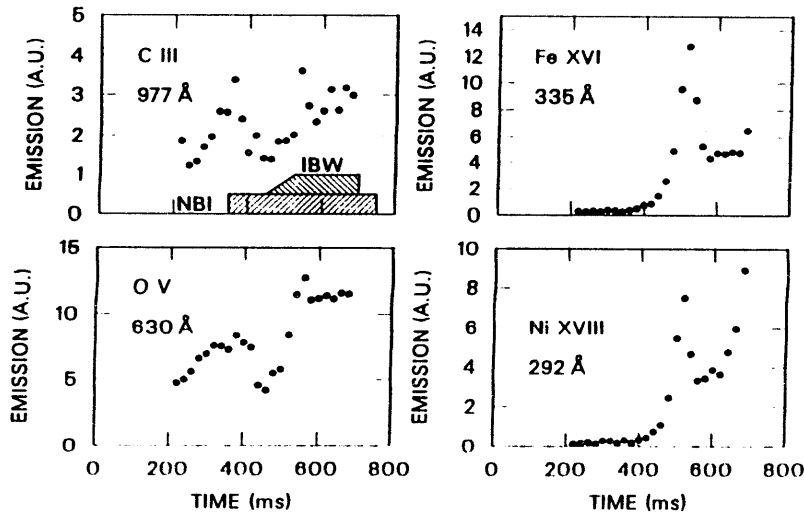


Fig. 6. Evolution of spectral line radiation during IBWH in an H-mode plasma

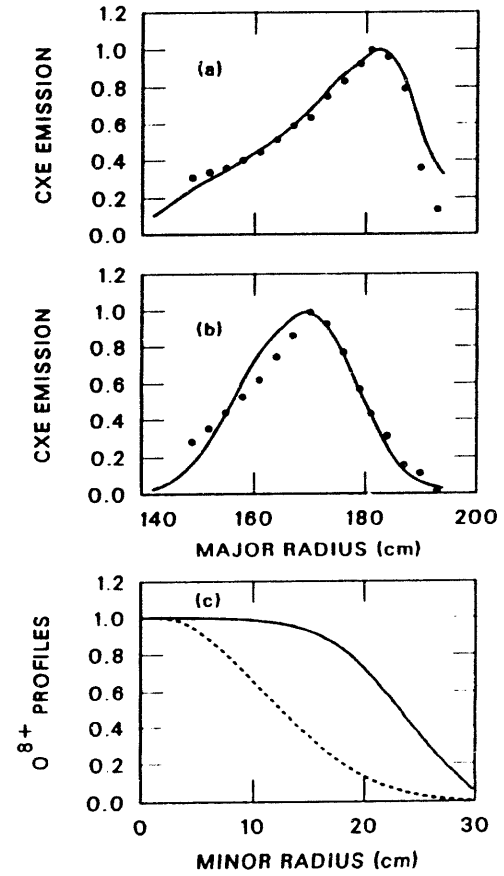


Fig. 7. CXE signals from the 2977 Å line of O⁷⁺, (a) H-mode with NBI only, (b) H-mode with IBW. (c) Profiles of fully ionized oxygen deduced from CXE signals: solid line - without IBWH; dashed line - with IBWH.

**DATE
FILMED**

10/24/94

END

